GSICS
GLOBAL SPACE-BASED INTER-CALIBRATION SYSTEM

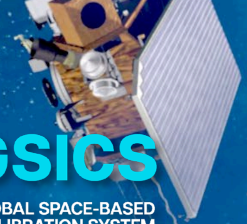

DOI: 10.25923/0x6x-ys07
Vol. 19 No 2, 2026

Quarterly

Newsletter Spring 2026 Issue

Associate Editor
Eric Robinson, NOAA Affiliate

WMO • EUMETSAT • NOAA • CMA • CNES • ESA • IMD • ISRO • JAXA • JMA • KMA • NASA • NIST • ROSCOSMOS • ROSHYDROMET • SITP • USGS

Articles

News in This Quarter

Announcements

GSICS-Related Publications

NOAA's Newest Satellite: SOLAR-1

By Dimitrios Vassiladis (NOAA)

The Space weather Observations at Lagrange 1 to Advance Readiness-1 (SOLAR-1; formerly: Space Weather Follow On – Lagrange 1, or SWFO-L1) mission of the National Oceanic and Atmospheric Administration (NOAA) was developed in collaboration with NASA with the goal of supplying solar coronal images and solar wind measurements to NOAA's National Weather Service (NWS) and other users. The mission has started providing critical data that will enable the monitoring and prediction of space weather events near Earth before they can impact technological systems. SOLAR-1 will replace NOAA's Deep Space Climate Observatory (DSCOVR) and the operational functions of NASA's Solar and Heliospheric Observatory (SoHO) and Advanced Composition Explorer (ACE).

The SWFO-L1 spacecraft was launched on September 24, 2025 from Kennedy Space Center on a SpaceX Falcon 9 rocket together with NASA's Interstellar Mapping and Acceleration (IMAP) and Carruthers Geocoronal Observatory. The spacecraft traveled to the Sun-Earth Lagrange 1 (L1) point from which it will send coronal images and *in situ* measurements to Earth (Fig. 1). The Lagrange Orbit Insertion (LOI) maneuvers were completed on January 27, 2026 and the mission was renamed SOLAR-1 at that time. The spacecraft has both remote-sensing and in situ capabilities: It carries the Compact Coronagraph-2 (CCOR-2), developed by the Naval Research Laboratory (NRL; PI: A. Thernisien) to image the solar corona and detect coronal mass ejections (CMEs), the powerful drivers of the most intense geomagnetic storms [1]. Its Solar Wind Plasma Sensor (SWiPS), developed by the Southwest Research Institute (SwRI; PI: R. Ebert) measures the velocity distribution function of protons and alpha particles from which the speed, density, temperature, and pressure are calculated [2]. The magnetometer (MAG) suite of two fluxgate sensors, developed by the University of New Hampshire and SwRI (PI: R. Torbert) measures the interplanetary magnetic field (IMF), a crucial space weather variable, with a cadence of 64 vectors/s [3]. Complementing SWiPS, the SupraThermal Ion Sensor (STIS), developed by the University of California, Berkeley (PI: D. Larson) measures the suprathermal ion (25 keV-6 MeV) and electron (25-300 keV) populations which are important precursors of solar energetic particles (SEPs) and are well correlated with the K_p index representing the average geomagnetic disturbance level [4].

SOLAR-1 is the second component of NOAA's broader Space Weather Follow On (SWFO) program, the first being a solar telescope: the Compact Coronagraph-1 (CCOR-1) was launched on June 25, 2024, onboard NOAA's Geostationary Operational Environmental Satellite-19 (GOES-19) and provides a backup capability to CCOR-2.

The National Environmental Satellite Data and Information Service (NESDIS) has built a ground segment to support SOLAR-1 including a network of six antenna stations around the globe to ensure continuous downlink from L1. To provide further resiliency, international partners such as Japan's National Institute of Information and Communications Technology (NICT) and Korea's Korean Space Weather

DOI: 10.25923/0x6x-ys07

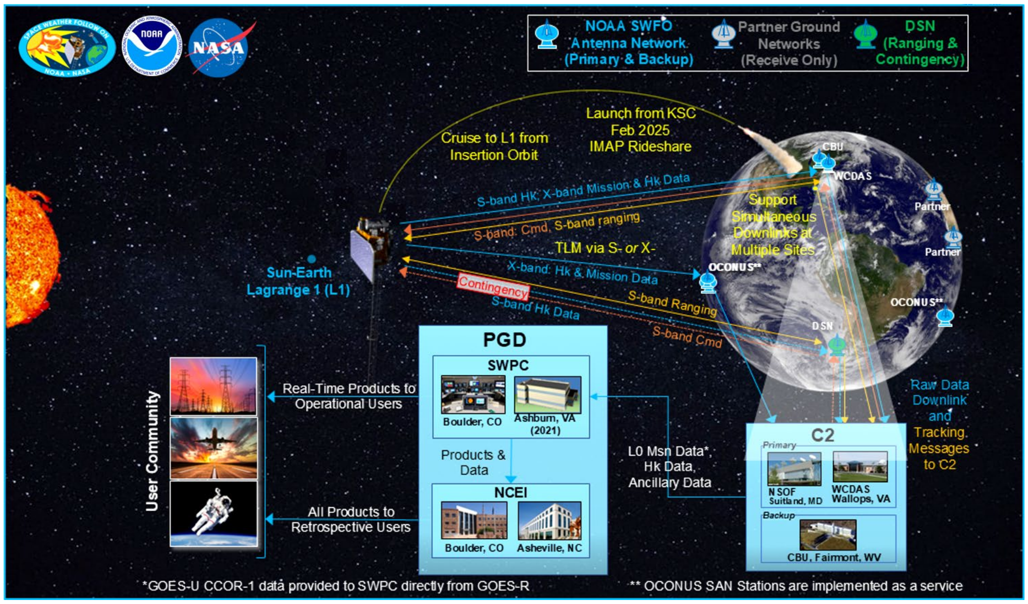

Figure 1. Concept of Operations (CONOPS) schematic for the SOLAR-1 mission at the Sun-Earth L1 point.

Center (KWTC) will track the satellite for NOAA. CCOR-1 and SOLAR-1 data are processed into operational products by the Space Weather Prediction Center (SWPC) of NWS and are made available in near-real time (https://www.swpc.noaa.gov/products-and-data) to SWPC's forecast center and other meteorological agencies, and other users; and into retrospective products by the National Centers for Environmental Information (NCEI).

The coronal images, solar wind velocity, and IMF are Key Performance Parameters (KPPs) of the SWFO program, and together with other data are used in issuing alerts, warnings, and watches, and in driving real-time numerical weather prediction (NWP) models [4; 5], analysis tools [6] at SWPC and in other operational centers [7]. Both sets of data are archived at the NESDIS Common Cloud Framework (NCCF) and are freely available through NCEI's Space Weather Portal (SPOT; https://www.ncei.noaa.gov/products/space-weather) for further research and development. SWFO is a program at the NESDIS office of Space Weather Observations (SWO) and additional information on its requirements, instruments, and publications is available (https://www.nesdis.noaa.gov/our-satellites/future-programs/swfo/swfo-data-products-and-science).

In terms of intercalibration and the activities planned by the GSICS Space Weather group, the presence of six spacecraft with similar instrumentation around L1 is unprecedented [8]. In addition to SOLAR-1 and IMAP, the Indian Space Research Organization's (ISRO) Aditya-L1 launched in September 2023 and joined the legacy solar wind monitors ACE, DSCOVR, and Wind. Four of the spacecraft are in narrower Lissajous orbits while Aditya-L1 and Wind are in wider, elliptical "halo" orbits. Comparisons with IMF measurements from ACE, DSCOVR, and IMAP have been undertaken and shown excellent prospects for gain calibration. After calibration procedures have been finalized, the differences between the magnetometer measurements will be useful for understanding the 3D structure of events at a broad range of spatial scales ranging from CMEs to switchbacks and waves. Similar intercalibration is planned for plasma and particle sensors.

Similarly, CCOR-1 images are being intercalibrated with those from SoHO's Large Angle and Spectrographic Coronagraph (LASCO), specifically the C3 telescope and the same calibration will happen with CCOR-2 images. CCOR-1 images are superior in dynamic range, angular resolution, image saturation, signal-to-noise (S/N) ratio, suppression of SEPs, and other aspects while similar in cadence and with a reduced, as deemed practical, field of view (FOV). Comparisons are planned with other coronagraphs such as the Multi-Element Telescope for Imaging and Spectroscopy (METIS) onboard ESA's Solar Orbiter, with the first joint observations in Nov. 2024 and Oct. 2025, and the Narrow Field Imager (NFI) onboard NASA's Polarimeter to Unify the Corona and Heliosphere (PUNCH).

SOLAR-1 together with CCOR-1 implements the NOAA vision of providing critical solar and interplanetary data to operational users

DOI: 10.25923/0x6x-ys07

and the global space weather community. These activities will enable a continuous and improved awareness of space environmental conditions.

References

1. Thernisien, A., Chua, D., Carter, T., Rich, N., Noya, M., & Babich, T. . (2026). The CCOR compact coronagraphs for GOES-19 and the Space Weather Follow On missions *[Manuscript accepted]. Space Science Reviews*.
2. Ebert, R. W., Mokashi, P. S., Carey, J., Barr, D. A., Blase, R. C., Candelaria, J., Coon, S. J., Dennis, G. C., Elder, H. A., Escobedo, S. M., Ertley, C. D., Fortenberry, M. L., Friday, J. M., Gomez, R. G., Gonzales, E. S., Grubbs II, G. A., Hoffmeyer, M. M., Llera, K., Mello, K.,…Valek, P. W. (2026). The Solar Wind Plasma Sensor (SWiPS) on NOAA's Space Weather Observations at L1 to Advance Readiness – 1 (SOLAR-1) mission *[Manuscript submitted]. Space Science Reviews*.
3. Torbert, R. B., Dors, I., Argall, M. R., Smith, C., Fischer, D., Magnes, W., Vaith, H., Abel, D., Cardarelli, G., Frost, C., Vasquez, B., Marhefka, F., & Valavanoglou, A. . (2026). The magnetometer on SWFO-L1 *[Manuscript accepted]. Space Science Reviews*.
4. Rahmati, A., Larson, D. E., Jolitz, R., Dunn, P., Abono, C., Mercer, T., et al. (2026). The SupraThermal Ion Sensor (STIS) onboard the Space Weather Follow On Lagrange-1 (SWFO-L1) mission *[Manuscript submitted]. Space Science Reviews*.
5. Glocer, A., Rastätter, L., Kuznetsova, M., Pulkkinen, A., Singer, H. J., Balch, C., Weimer, D., Welling, D., Wiltberger, M., Raeder, J., Weigel, R. S., McCollough, J., & Wing, S. (2016). Community-wide validation of geospace model local K-index predictions to support model transition to operations. *Space Weather*, *14*(7), 469-480. DOI:10.1002/2016SW001387
6. Fang, T. W., Kubaryk, A., Goldstein, D., Li, Z., Fuller-Rowell, T., Millward, G., Singer, H. J., Steenburgh, R., Westerman, S., & Babcock, E. (2022). Space Weather Environment During the SpaceX Starlink Satellite Loss in February 2022. *Space Weather*, *20*(11). DOI:10.1029/2022sw003193
7. Millward, G., Biesecker, D., Pizzo, V., & de Koning, C. A. (2013). An operational software tool for the analysis of coronagraph images: Determining CME parameters for input into the WSA-Enlil heliospheric model. *Space Weather*, *11*(2), 57-68. DOI:10.1002/swe.20024
8. Tsagouri, I., Belehaki, A., Bergeot, N., Cid, C., Delouille, V., Egorova, T., Jakowski, N., Kutiev, I., Mikhailov, A., & Núñez, M. (2013). Progress in space weather modeling in an operational environment. *Journal of Space Weather and Space Climate*, *3*, A17. DOI:10.1051/swsc/2013037
9. Turner, D., Horbury, T., Vassiliadis, D., Ebert, R., Wilson, L., Christian, E., Szabo, A., Chakrabarty, D., Rankin, J., Gkioulidou, M., & McComas, D. (2026). *IMAP and the L1 Constellation: Unprecedented insights on the 3-dimensional structure and spatiotemporal evolution of the solar wind near 1 astronomical unit* COSPAR, Florence.

Exploring the Value of Spire GNSS Radio Occultation Data for Improving NOAA's Hurricane Model Forecasts

By William J. Miller (UMD), Yong Chen (NOAA), Shu-Peng Ho (NOAA), and Xi Shao (UMD)

Global Navigation Satellite System (GNSS) radio occultation (RO) observations are an essential data source, providing high-vertical-resolution profiles of temperature and water vapor. These nearly unbiased observations, accurate above the boundary layer, complement satellite radiances [1].The high quality of RO data also makes them a highly stable reference for the calibration and validation of satellite radiance observations, acting as a robust data source for infrared and microwave sounder calibration efforts [2]. When assimilated as bending angles or refractivity, RO data have been shown to improve forecast model skill in predicting TC development and intensification [3;4]. Currently, most GNSS RO observations assimilated in current weather forecasting models primarily come from government-owned RO receiver satellite missions such as the US-Taiwan Constellation Observing System for Meteorology, Ionosphere, and Climate-2 (COSMIC-2). These missions provide fewer than 10,000 profiles per day globally, resulting in spotty and inconsistent coverage near TCs [4].

To address this gap, a recently published observing simulation experiment (OSE) study by NOAA STAR-affiliated scientists [5] investigated the impacts of assimilating commercial GNSS RO observations provided by Spire Global, Inc. (hereafter Spire) in NOAA's Hurricane Weather Research and Forecasting (HWRF) model. Except for GNSS RO data, all current operational satellite measurements, including microwave, infrared, and in situ data, were also included in the OSE. The authors selected four Atlantic hurricanes from the 2022 season – Earl, Fiona, Ian, and Julia, and ran three independent HWRF cycled data assimilation

DOI: 10.25923/0x6x-ys07

experiments covering the TC lifecycles. A Control experiment assimilated only a small amount of operational RO data; for the C2 experiment, COSMIC-2 data were added, and the C2SPIRE experiment also assimilated Spire RO bending angles purchased by NOAA's Commercial Data Program for evaluation. The Spire dataset contained about 5,500 daily global RO profiles, providing up to four additional profiles for assimilation per cycle in HWRF's inner storm-following nest. Their HWRF model used a one-dimensional forward operator [6] to generate bending angles from the background meteorological fields

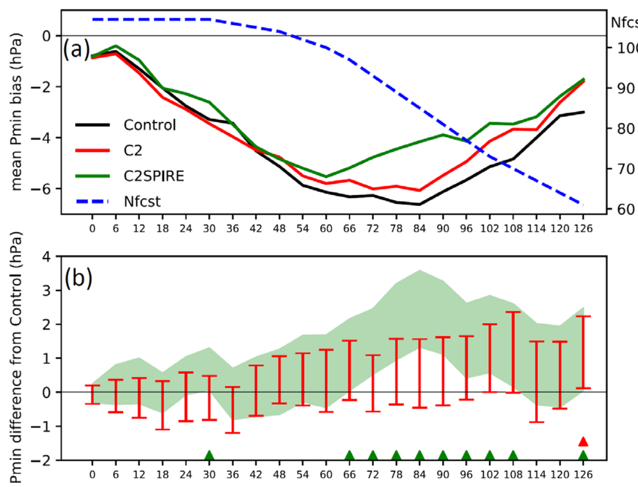

Figure 1. (a) Time series of mean HWRF P_{MIN} intensity bias (hPa) for Control (black line), C2 (red line), and C2SPIRE (green line). The dashed blue line shows the number of forecasts evaluated. (b) Green shading (red bars) denotes the 90% confidence interval of the C2SPIRE-minus-Control (C2-minus-Control) forecast P_{MIN} error differences (hPa) generated by bootstrap resampling sets of forecast pairs (1000 iterations). Green (red) triangles mark times when C2SPIRE (C2) has a statistically significant smaller absolute P_{MIN} bias compared to Control.

along a vertical column extending upward from the ray perigee point to the top of the atmosphere. In addition to their HWRF forecast verification, Miller et al. [5] also evaluated the assimilated Spire RO data quality. Compared to COSMIC-2, the Spire GNSS RO receiver antenna is about 50% shorter, and therefore, it is important to determine whether the accuracy and precision of Spire RO data are adequate for weather forecasting applications. Ho et al. [7] showed that despite Spire's lower mean signal-to-noise ratio (SNR), differences in the two missions' receiver antenna geometries results in Spire's SNR being latitudinally invariant, while COSMIC-2's SNR is smallest in the midlatitudes, which likely explains why their evaluated Spire profiles tended to penetrate deeper into the lower troposphere poleward of 30° N and 30°S compared to COSMIC-2. Miller et al. [5] analyzed RO observation-minus-background (O – B) and observation-minus-analysis (O – A) statistics from their C2SPIRE experiment. Additionally, they diagnosed RO observation errors (that implicitly include instrument and retrieval sources) using the Desroziers et al. [8] method, which estimates the diagonal elements of an observation error matrix as the expectation of the O – B and O – A matrix product.

Key findings from Miller et al. [5] are:

- Assimilating the Spire data yielded a statistically significant 17% - 38% reduction in the mean bias of Control's minimum central sea-level pressure (P_{MIN}) intensity for medium-to-long range forecasts (Figure 1).
- C2SPIRE's reduced over-intensification bias was consistent with modest lower tropospheric drying caused by Spire assimilation for some cases evaluated (Figure 2).

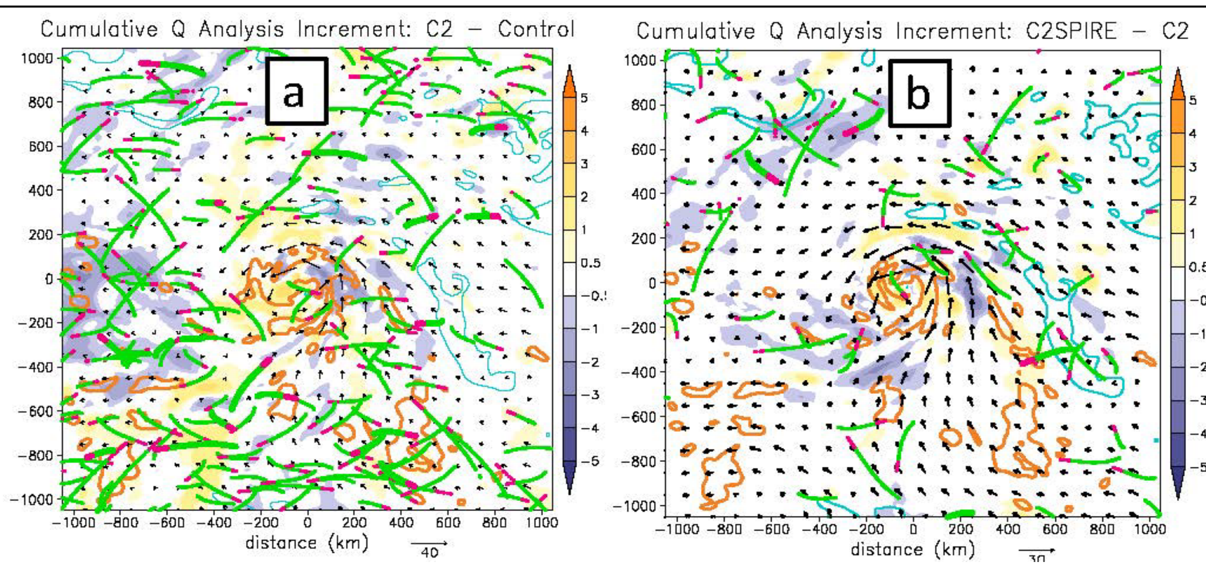

Figure 2. HWRF specific humidity analysis increments (shaded; g kg^{-1}) averaged over the 850-950 hPa layer and accumulated over the first 60 hours of the cycled Hurricane Earl (2022) experiments, shown as C2-minus-Control differences in (a) and C2SPIRE-minus-C2 in (b). The t = 60 h, 900 hPa horizontal wind vectors (m s^{-1}) and specific humidity (15 and 11 g kg^{-1} contours shown in orange and blue, respectively) are also shown for (a) C2 and (b) C2SPIRE. COSMIC-2 and Spire profiles assimilated over this 60-h period are shown as green swaths in (a) and (b), respectively, with magenta tips showing the portions of the profiles extending below 800 hPa.

DOI: 10.25923/0x6x-ys07

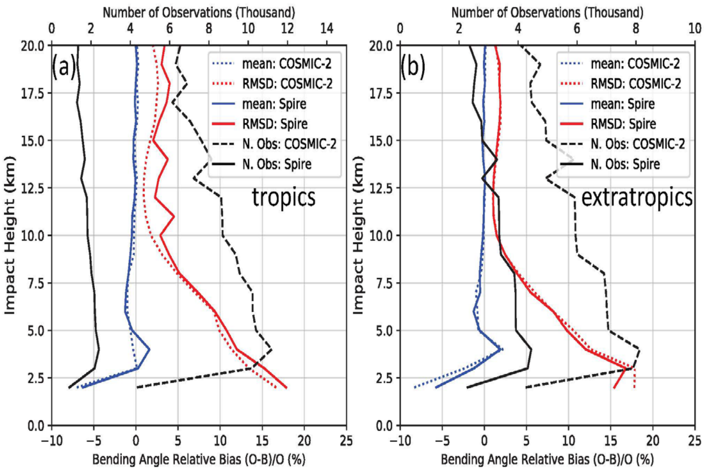

Figure 3. Profiles of the Spire (solid lines) and COSMIC-2 (dotted lines) normalized O-B statistics derived from all C2SPIRE analyses for the (a) tropics and (b) extratropics poleward of 20 degrees N. Normalized O-B mean and RMSD profiles are shown in blue and red, respectively.

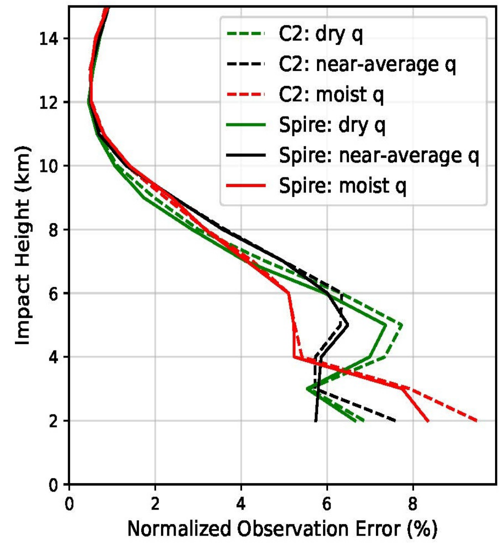

Figure 4. (a) Spire (solid) and COSMIC-2 (dashed) normalized bending angle observation error standard deviation profiles diagnosed from C2SPIRE O-B and O-A data for observations binned by background specific humidity for moist (green), near-average (black), and dry (green) regimes relative to climatology. Normalized O-B mean and RMSD profiles are shown in blue and red, respectively.

- Compared to Control, short-range C2SPIRE forecast temperature and specific humidity root-mean-square errors (RMSEs) measured against dropsondes released by NOAA hurricane hunter aircraft were ~5-10% smaller in the lower troposphere.
- Spire had a smaller O – B RMSE than COSMIC-2 in the extratropical lower troposphere (Figure 3b), consistent with Ho et al. [7]'s reporting degradation in COSMIC-2's SNR in the midlatitudes due to its antenna geometry.
- Despite the Spire RO data having an overall lower signal-to-noise ratio compared to COSMIC-2, Spire's bending angle observation errors diagnosed from the C2SPIRE analysis and background departure statistics were comparable or smaller in the lower-to-middle troposphere with the largest differences near the boundary layer in moister environments (Figure 4).
- A smaller percentage of lower tropospheric Spire data was rejected by HWRF's quality control algorithm, compared to COSMIC-2.

In conclusion, the Miller et al. [5] study provides compelling evidence that assimilating commercial Spire GNSS RO observations leads to meaningful improvements in HWRF intensity forecasts, significantly reducing the mean over-intensification bias for the hurricanes evaluated. Additionally, Spire data were found to be of similar or higher quality than COSMIC-2 in the lower troposphere, where water vapor effects increase the uncertainty in RO data retrieval [9]. This success highlights the value of commercial data in complementing government missions. Future work will focus on conducting additional OSEs to validate these results for a larger set of hurricane cases. Furthermore, ongoing optimization of GNSS RO observation error specification, quality control, and forward operator accuracy in NOAA's hurricane forecasting models remains a priority, particularly for the lower troposphere, where observation uncertainty is higher, and the impact on TC forecasts is critical.

References

1. Ho, S.-p., Anthes, R. A., Ao, C. O., Healy, S., Horanyi, A., Hunt, D., Mannucci, A. J., Pedatella, N., Randel, W. J., Simmons, A., Steiner, A., Xie, F., Yue, X., & Zeng, Z. (2020). The COSMIC/FORMOSAT-3 Radio Occultation Mission after 12 Years: Accomplishments, Remaining Challenges, and Potential Impacts of COSMIC-2. *Bulletin of the American Meteorological Society*, *101*(7), E1107-E1136. DOI:10.1175/BAMS-D-18-0290.1

2. Zou, X., Lin, L., & Weng, F. (2014). Absolute Calibration of ATMS Upper Level Temperature Sounding Channels Using GPS RO Observations. *IEEE Transactions on Geoscience and Remote Sensing*, *52*, 1397-1406. DOI:10.1109/tgrs.2013.2250981

3. Chen, S.-Y., Kuo, Y.-H., & Huang, C.-Y. (2020). The Impact of GPS RO Data on the Prediction of Tropical Cyclogenesis Using a Nonlocal Observation Operator: An Initial Assessment. *Monthly Weather Review*, *148*(7), 2701-2717.

DOI:10.1175/MWR-D-19-0286.1

4. Miller, W. J., Chen, Y., Ho, S.-P., & Shao, X. (2023). Evaluating the Impacts of COSMIC-2 GNSS RO Bending Angle Assimilation on Atlantic Hurricane Forecasts Using the HWRF Model. *Monthly Weather Review*, *151*(7), 1821-1847. DOI:10.1175/MWR-D-22-0198.1
5. Miller, W. J., Chen, Y., Ho, S.-P., & Shao, X. (2025). Exploring the Value of Spire GNSS Radio Occultation Bending Angle Assimilation for Improving HWRF Model Forecasts of Atlantic Hurricane Intensity. *Weather and Forecasting*, *40*(6), 809-827. DOI:10.1175/WAF-D-24-0092.1
6. Cucurull, L., Derber, J. C., & Purser, R. J. (2013). A bending angle forward operator for global positioning system radio occultation measurements. *Journal of Geophysical Research: Atmospheres*, *118*(1), 14-28. DOI:10.1029/2012JD017782
7. Ho, S.-p., Zhou, X., Shao, X., Chen, Y., Jing, X., & Miller, W. (2023). Using the Commercial GNSS RO Spire Data in the Neutral Atmosphere for Climate and Weather Prediction Studies. *Remote Sensing*, *15*(19), 4836. DOI:10.3390/rs15194836
8. Desroziers, G., Berre, L., Chapnik, B., & Poli, P. (2005). Diagnosis of observation, background and analysis-error statistics in observation space. *Quarterly Journal of the Royal Meteorological Society*, *131*(613), 3385-3396. DOI:10.1256/qj.05.108
9. Kursinski, E. R., Hajj, G. A., Schofield, J. T., Linfield, R. P., & Hardy, K. R. (1997). Observing Earth's atmosphere with radio occultation measurements using the Global Positioning System. *Journal of Geophysical Research: Atmospheres*, *102*(D19), 23429-23465. DOI:10.1029/97JD01569

Assessment of Next-Generation Microwave Sounders: Information Content and Calibration Implications

By Flavio Iturbide-Sanchez (NOAA), and Eric Maddy (ERT)

Introduction

Emerging microwave sounding technologies are reshaping the architecture of space-based atmospheric observations. Advances in reduced size, weight, and power (SWaP) have enabled compact, cost-effective microwave radiometers suitable for CubeSats and small satellite platforms. These systems support distributed constellations capable of providing improved temporal sampling compared to traditional single-platform missions. Next-generation microwave sounders are expanding spectral coverage beyond current operational systems (such as NOAA's Advanced Technology Microwave Sounder - ATMS which spans 23.8–183.31 GHz across 22 channels. New missions introduce additional absorption bands and higher spectral resolution channels designed to improve thermodynamic and hydrometeor profiling, cloud and precipitation sensitivity, and near-surface moisture retrievals. This study evaluates the information content and geophysical retrieval performance of several emerging microwave sounders, including commercial systems supported under NOAA's Commercial Data Program, relative to ATMS. Artificial intelligence (AI) techniques are applied to enable scalable performance assessment across diverse sensor configurations. Results provide guidance for integrating commercial and international microwave observations into NOAA's evolving observing system and inform GSICS inter-calibration and validation priorities.

Background

Recent missions are expanding spectral capabilities beyond traditional 50–60 GHz oxygen and 183 GHz water vapor bands.

- NASA's Time-Resolved Observations of Precipitation structure and storm Intensity with a Constellation of Smallsats (TROPICS) [1] and the commercial Tomorrow.io Microwave Sounder (TMS) [2] missions employ the 118.75 GHz oxygen absorption band for temperature sounding, deploying compact microwave sounders optimized for distributed coverage.
- The European Space Agency (ESA)'s Arctic Weather Satellite (AWS) [3] exploits the 325.15 GHz water vapor absorption line to enhance moisture and cloud sensitivity, particularly in high-latitude regions.
- Some next generation concepts incorporate ~205 GHz or 229 GHz channels to improve sensitivity to ice scattering, near-surface water vapor, and surface emissivity.

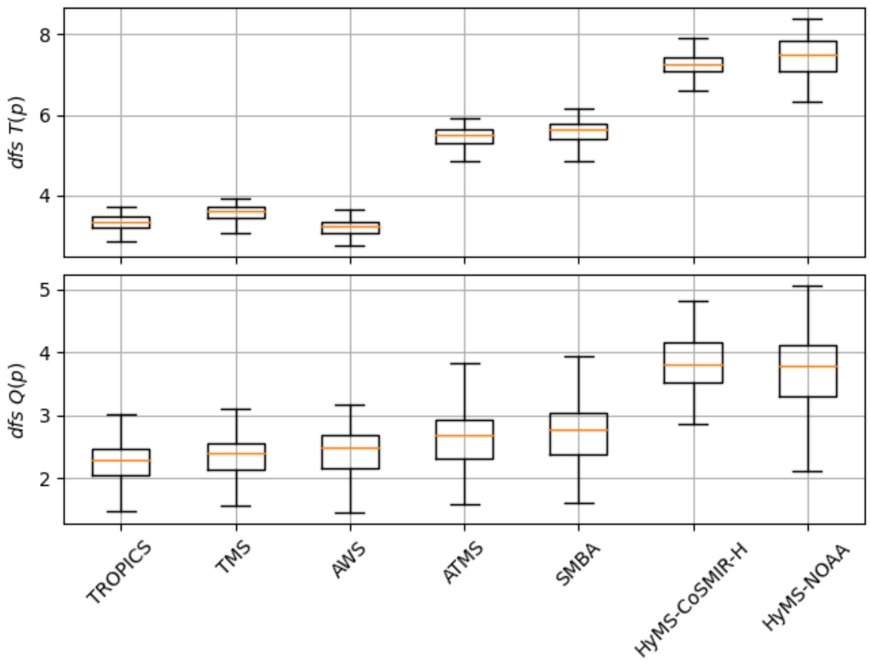

Figure 1. Information content for atmospheric temperature (top) and water vapor (bottom) retrievals, quantified using degrees of freedom for signal (DFS) under all-sky conditions. Results are shown for ATMS and selected next-generation microwave sounders. Boxes and whiskers represent the variability in DFS computed over a set of profiles representing expected atmospheric variability in temperature, moisture, surface and cloud conditions [5].

The 118 GHz band complements the 50–60 GHz oxygen complex by providing additional vertical resolution in the troposphere. However, instruments lacking high-peaking 50–60 GHz or 118 GHz channels may experience reduced stratospheric temperature sensitivity. Hyperspectral Microwave Sounder (HyMS) concepts extend this evolution further by providing dense spectral sampling across microwave and sub-millimeter bands. High spectral resolution and low instrument noise are expected to increase information content in the microwave observations, while improving resilience to radio-frequency interference (RFI) through enhanced spectral redundancy [4]. By measuring overlapping portions of the microwave spectrum at high spectral resolution, these hyperspectral instruments also can provide a high spectral resolution calibration reference for operational microwave sensors such as ATMS, enabling validation of instrument spectral response and spectral calibration accuracy.

The reduced SWaP of modern sensors enables deployment in distributed constellations, increasing temporal resolution and system resilience. However, small platforms often trade reduced spectral coverage for cost and deployment flexibility, factors directly relevant to GSICS inter-calibration consistency.

For microwave temperature and moisture sounders, information-content and retrieval performance studies provide the key radiance-to-impact link for GSICS calibration/validation. Information-content diagnostics identify which channels and layers are truly constrained by observations versus dominated by background or prior information, ensuring that inter-calibration efforts focus on regions where the instrument has true physical sensitivity. Retrieval assessments show whether inter-sensor radiance corrections actually reduce uncertainties in downstream applications. Together, these tools can sharpen detection of slow radiometric drift, reduce false “calibration” signals caused by representativeness/scene variability, and support more consistent long-term records and use in operational systems.

Information Content Analysis

Information content was evaluated using a Bayesian inverse framework, with degrees of freedom for signal (DFS) computed for temperature and water vapor under all-sky conditions [5]. In this study, ATMS was used as the reference system.

Results shown in **Figure 1** indicate:

- Tomorrow.io TMS exhibits reduced temperature DFS relative to ATMS, primarily due to higher instrument noise and absence of high-peaking channels needed for stratospheric sensitivity.
- ESA AWS shows similarly reduced stratospheric temperature sensitivity for the same reason.
- For water vapor, TMS provides DFS comparable to ATMS in portions of the troposphere, though sensitivity differences emerge near the surface due to the absence of low-frequency channels (e.g., 23.8 GHz).
- A notional Sounder for Microwave-Based Applications (SMBA) [6], incorporating 50 GHz, 118 GHz, and 229 GHz bands, demonstrates modest improvements in both temperature and water vapor DFS relative to ATMS. The 118 GHz band provides redundancy that effectively reduces noise through combined information with 50 GHz channels.
- The HyMS concepts, based on NASA’s CoSMIR-H [7] and NOAA notional designs [4], consistently

DOI: 10.25923/0x6x-ys07

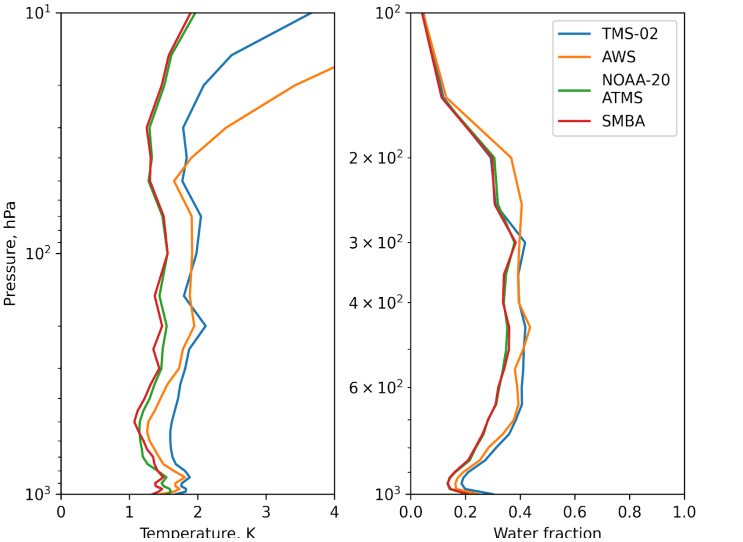

Figure 2a. MIIDAPS-AI temperature (left) and moisture (right) vertical profile statistics computed over the independent validation dataset for NOAA-20 ATMS, Tomorrow.io TMS-02, SMBA, and ESA AWS microwave sounders. Root-mean-squared error, RMSE, computed as the difference between MIIDAPS-AI for each sensor and FV3GFS truth profiles. Temperature is reported as an absolute error, while water is reported as a relative difference from the mean of the FV3GFS true profiles under global all-sky conditions.

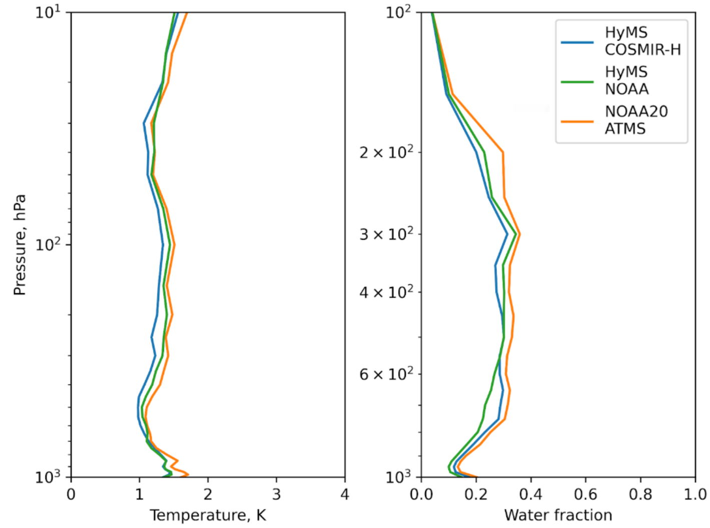

Figure 2b. MIIDAPS-AI temperature (left) and moisture (right) vertical profile statistics computed over the independent validation dataset for simulated observations of NOAA-20 ATMS and hyperspectral microwave sounders, including NASA CoSMIR-H and notional HyMS NOAA. Root-mean-squared error, RMSE, computed as the difference between MIIDAPS-AI for each sensor and FV3GFS truth profiles. Temperature is reported as an absolute error, while water is reported as a relative difference from the mean of the FV3GFS true profiles under global all-sky conditions.

show increased DFS for both temperature and water vapor due to:

- Low noise equivalent differential temperature (NEDT)
- Dense spectral sampling
- Broad spectral coverage

Geophysical Assessment

Atmospheric retrieval performance was evaluated using the Multi-Instrument Inversion and Data Assimilation Preprocessing System-Artificial intelligence (MIIDAPS-AI) system [4, 5, 8], a deep neural network trained and validated under global, all-weather conditions. Simulated observations were generated using NOAA-20 ATMS orbital geometry matched with FV3-GFS model output and fed into sensor-specific Community Radiative Transfer Model (CRTM) for consistency across sensors. Instrument noise equivalent delta temperature (NEDT) was then added to the ideal, noise free simulations. MIIDAPS-AI retrieval errors were computed relative to the NOAA FV3-GFS model, used here as a proxy reference for relative sensor comparison.

Key findings reported in **Figure 2** are consistent with information content assessments and show:

Temperature profiling

- TMS and AWS exhibit limitations in temperature profiling, particularly near and above the stratosphere, due to reduced information content in these regions.
- SMBA provides improvement relative to ATMS owing to the inclusion of the 118 GHz band and the resulting reduction in effective noise. Error reductions are observed both below 50 hPa and within the 100–500 hPa pressure range, with improvements of less than 1 K below 50 hPa and about 1 K in the 100–500 hPa tropospheric layer.
- HyMS sensors demonstrate the strongest improvement across most atmospheric layers.

Water vapor profiling

- Performance degradation in TMS and AWS is linked to:
  - Absence of ~23 Ghz channels for near-surface humidity
  - Reduced effective signal-to-noise ratio (S/N) in 183 GHz channels (particularly for AWS)
- TMS includes fewer 183 GHz channels than ATMS, reducing vertical moisture resolution.
- HyMS provides the most consistent improvement due to low noise and enhanced spectral sampling.

These results reinforce that comprehensive sampling of key microwave absorption bands, together with low instrument noise, strongly determines thermodynamic profiling capability.

Conclusions

Enabled by low-SWaP architectures, expanded spectral coverage, and distributed constellations, next-generation microwave sounding technologies offer significant opportunities to enhance NOAA's Earth observing system. This study highlights that:

- Instrument spectral coverage, noise performance, and channel configuration strongly control temperature and water vapor information content.
- The absence of high-peaking channels within the 50–60 GHz oxygen complex (or 118GHz oxygen line) significantly reduces sensitivity to upper-tropospheric and stratospheric temperature.
- The lack of low-frequency window channels (e.g., ~23–31 GHz) limits sensitivity to near-surface humidity and degrades moisture retrieval performance.
- Elevated instrument noise reduces effective DFS, diminishing retrieval accuracy even when appropriate spectral bands are included.

The notional SMBA configuration shows measurable improvement over ATMS through combined use of 50, 118, and 229 GHz bands. Hyperspectral microwave sounder concepts consistently show the largest potential performance gains due to low radiometric noise, dense spectral sampling, and broad spectral coverage.

These findings carry important implications for GSICS calibration and inter-calibration activities. Well calibrated hyperspectral observations, measuring overlapping frequencies with existing sensors, should enable cross-calibration of the spectral response stability and accuracy of traditional backbone sensors such as the ATMS. However, increasing spectral diversity across commercial and international constellations complicates direct channel-to-channel radiometric comparison and increases reliance on forward radiative transfer modeling to achieve cross-platform intercomparisons. When performed using real observations, AI-based retrievals such as MIIDAPS-AI do not require the use of a forward model [8], and can provide an independent "closure test" on inter-calibration quality and expected impact on downstream applications such as numerical weather prediction (NWP).

As NOAA diversifies its observing portfolio, rigorous radiometric characterization, noise assessment, and cross-spectral inter-calibration methodologies will be essential to ensure that enhanced temporal coverage and constellation resilience are achieved without compromising radiometric consistency or data integrity.

References

1. Blackwell, W. J., Braun, S., Bennartz, R., Velden, C., DeMaria, M., Atlas, R., Dunion, J., Marks, F., Rogers, R., Annane, B., & Leslie, R. V. (2018). An overview of the TROPICS NASA Earth Venture Mission. *Quarterly Journal of the Royal Meteorological Society*, *144*(S1), 16-26. DOI:10.1002/qj.3290
2. Slagen, D. (2024). Tomorrow.io's Microwave Sounder Satellites Capture Critical Atmospheric Insights [Web Article]. https://www.tomorrow.io/blog/tomorrow-ios-microwave-sounder-satellites-capture-critical-atmospheric-insights/
3. ESA. Introducing the Arctic Weather Satellite.
4. Maddy, E. S., Iturbide-Sanchez, F., & Boukabara, S. A. (2024). Toward the Next Generation of Microwave Sounders: Benefits of a Low-Earth Orbit Hyperspectral Microwave Instrument in All-Weather Conditions Using AI. *IEEE Journal of Selected Topics in Applied Earth Observations and Remote Sensing*, *17*, 4235-4246. DOI: 10.1109/jstars.2024.3356858
5. Maddy, E. S., & Iturbide-Sanchez, F. (2025). Next-Generation Satellite Architecture Planning-Scientific Arguments for Fusing Hyperspectral Microwave/Infrared Data Using Machine Learning. *IEEE Journal of Selected Topics in Applied Earth Observations and Remote Sensing*, *18*, 26081-26093. DOI:10.1109/jstars.2025.3605021
6. NASA. (2023). Sounder for Microwave-Based Applications (SMBA) Phase A Study. In: SAM.gov.
7. Kroodsma, R., Adams, I., Ames, T., Fritts, M., Gambacorta, A., Kotsakis, A., Mohammed, P., & Piepmeier, J. (2024). *COSMIR-H: An airborne hyperspectral microwave sounder for thermodynamic sensing of the planetary boundary layer* IEEE International Geoscience and Remote Sensing Symposium, Athens, Greece. https://2024.ieeeigarss.org/view_paper.php?PaperNum=3716
8. Maddy, E. S., & Boukabara, S. A. (2021). MIIDAPS-AI: An Explainable Machine-Learning Algorithm for Infrared and Microwave Remote Sensing and Data Assimilation Preprocessing - Application to LEO and GEO Sensors. *IEEE Journal of Selected Topics in Applied Earth Observations and Remote Sensing*, *14*, 8566-8576. DOI:10.1109/jstars.2021.3104389

DOI: 10.25923/0x6x-ys07

News In This Quarter

NOAA and EUMETSAT Technical Exchange Meeting on MetOp-SG Calibration/Validation

By Yong Chen (NOAA)

On March 12, 2026, NOAA and EUMETSAT held a technical exchange meeting focusing on the Calibration and Validation (Cal/Val) of the MicroWave Sounder (MWS) and Radio Occultation (RO) instruments during the evaluation period from December 16, 2025 to March 1, 2026. The presenters at the meeting highlighted the success of the MetOp-SG A1 mission and the strong partnership between NOAA and EUMETSAT.

Key highlights from the meeting:

- NOAA team members congratulated EUMETSAT on the successful launch of the MetOp-SG A1 and for the robust performance of the MWS and RO; they look forward to receiving data from the rest of the instruments.
- Cal/Val results from the NOAA team confirmed the excellent quality of the pre-operational MWS and RO observations.
- The meeting was very productive and the teams agreed to have a follow-up meeting in three months to continue our collaborative efforts.

Organized by Christophe Accadia of EUMETSAT, Satya Kalluri and Changyong Cao of NOAA, this technical exchange underscores a shared commitment to advancing Earth Observations for weather forecast and environmental monitoring through international cooperation.

Calibration/Validation Session at the 2026 AMS Annual Meeting

By Changyong Cao (NOAA)

The 106th AMS Annual Meeting, held from January 25 to 29, 2026, at the George R. Brown Convention Center in Houston, TX, provided an important platform for advancing the calibration/validation of satellite sensors. The Calibration/Validation (Cal/Val) for Environmental Remote Sensing and Numerical Weather Prediction (NWP) session took place within the Research to Operations (R2O) conference. Active participation from both in-person attendees and remote participants facilitated a robust technical exchange that highlighted the current state of satellite data quality assurance through Cal/Val.

The technical program showcased several advancements in the field, with emphasis on the growing role of commercial satellite constellations. Presenters discussed the rigorous protocols required to validate commercial data before its assimilation into operational NWP models, ensuring that these new data streams enhance forecast accuracy. Another major area was the Cal/Val for the MetOp-SG (Second Generation) mission. These discussions focused on early calibration results and the international collaboration necessary to optimize the performance of the next generation of polar-orbiting sensors. Several presentations introduced artificial intelligence and machine learning techniques as new tools in the Cal/Val of satellite products, including a new AI emulator for the CRTM (Community Radiative Transfer Model). The session was very successful and received positive feedback from peers.

2026 GSICS Annual and Executive Panel Meeting Held in Ottawa, Canada on March 23-27

By Eric Robinson (NOAA Affiliate)

The 2026 GSICS Annual and Executive Panel Meeting, co-organized by the National Research Council Canada and EUMETSAT, was held at the grounds of the National Research Council Canada. More information will follow in the summer newsletter edition.

Announcements

35th CALCON Technical Meeting Will Take Place on June 8-11, 2026 in Logan, Utah

Registration opens on April 1st and non-US Citizens must register before May 22nd. The meeting website can be found here.

The 2026 IEEE International Geoscience and Remote Sensing Symposium (IGARSS) to be held in Washington DC August 9-14

IGARSS 2026, the 46th annual conference of the IEEE Geoscience and Remote Sensing Society (GRSS) will be held at the Washington Hilton. Registration opens on April 1st, 2026. The meeting website can be found here.

GSICS-Related Publications

Doelling, D., Khakurel, P., Haney, C., Gopalan, A., & Bhatt, R. (2025). Regional Characterization of Deep Convective Clouds for Enhanced Imager Stability Monitoring and Methodology Validation. *Remote Sensing*, *17*(18), 3258. DOI:10.3390/rs17183258

He, X., Xu, N., Hu, X., Wang, L., Xi, H., He, Y., Chen, L., & Zhang, P. (2026). Consistency transfer calibration method for MERSI solar reflection bands of FY-3 series. *Measurement*, *269*, 120682. DOI:10.1016/j.measurement.2026.120682

Liang, X., Liu, Q., & Grassotti, C. (2026). Refining Clear-Sky AI Radiative Transfer Model Forward Predictions and Jacobian Accuracy for ATMS Using a ResNet and Physical Constraints. *IEEE Transactions on Geoscience and Remote Sensing*, *64*, 1-15. DOI:10.1109/TGRS.2026.3665759

Maddy, E. S., & Iturbide-Sanchez, F. (2025). Next-Generation Satellite Architecture Planning-Scientific Arguments for Fusing Hyperspectral Microwave/Infrared Data Using Machine Learning. *IEEE Journal of Selected Topics in Applied Earth Observations and Remote Sensing*, *18*, 26081-26093. DOI:10.1109/JSTARS.2025.3605021

Moradi, I., & Kalluri, S. (2025). ML-driven cross-calibration of microwave and infrared instruments. *Machine Learning: Earth*, *1*(1), 015012. DOI:10.1088/3049-4753/ae1cce

Venkatesulu, E., Duley, E., & Shaw, J. (2025). Visible and near-infrared Moon polarization across the lunar cycle. *Journal of Applied Remote Sensing*, *19*(4), 044502. DOI:10.1117/1.JRS.19.044502

Wang, L., Zhou, L., Sun, H., Burrow, C., Yan, B., & Kalluri, S. (2025). VIIRS Radiance Cluster Analysis in CrIS Observations for Enhanced Data Assimilation in NWP Models. *Earth and Space Science*, *12*(10), e2025EA004503. DOI:10.1029/2025EA004503

Wethey, D. S., Woodin, S. A., & Vazquez-Cuervo, J. (2026). On-Orbit Correction of ECOSTRESS Radiances by Comparison with IASI Hyperspectral Sounders. *Remote Sensing*, *18*(4), 622. DOI:10.3390/rs18040622

DOI: 10.25923/0x6x-ys07

Yan, B., Liang, D., Jin, X., Sun, N., Iturbide-Sanchez, F., Wu, X., & Wang, L. (2026). Long-Term Assessment of Inter-Sensor Radiometric Biases Among SNPP, NOAA-20, NOAA-21 OMPS Nadir, and CrIS Instruments Using the NOAA ICVS-iSensor-RCBA Portal. *Remote Sensing*, *18*(2), 254. DOI:10.3390/rs18020254

Yu, F., Wu, X., Yoo, H., Xu, H., & Qian, H. (2025). Direct Comparison of Infrared Channel Measurements by Two ABIs to Monitor Their Calibration Stability. *Remote Sensing*, *17*(10), 1656. DOI:10.3390/rs17101656

Zhu, S., Zhang, L., Xie, Y., Qie, L., Li, Z., Zhang, M., & Wang, X. (2025). In-Flight Radiometric Calibration of Gas Absorption Bands for the Gaofen-5 (02) DPC Using Sunglint. *Remote Sensing*, *17*(21), 3558. DOI:10.3390/rs17213558

Submitting Articles to the GSICS Quarterly Newsletter:

The GCC Quarterly has a new editorial staff. We would like to sincerely thank Manik Bali (UMD) for his excellent service as editor of the GSICS Quarterly for the last twelve years (Vol. 7 #3 through Vol. 19 #1)

The GSICS Quarterly Press Crew is looking for short articles (800 to 900 words with one or two key, simple illustrations), especially related to calibration / validation capabilities and how they have been used to positively impact weather and climate products. Unsolicited articles may be submitted for consideration anytime, and if accepted, will be published in the next available newsletter issue after approval / editing. Please send articles to eric.robinson@noaa.gov.

With help from our colleagues:

The GSICS Quarterly Editor would like to thank Lawrence Flynn (NOAA), Wenghui Wang, and Slawomir Blonski for reviewing articles in this issue. Thanks are due to Jan Thomas (NOAA) for helping with 508 compliance.

Published By

GSICS Coordination Center
NOAA/NESDIS/STAR
NOAA Center for Weather
and Climate Prediction,
5830 University Research Court
College Park, MD 20740, USA